Materials and Design 35 (2012) 589–595

Contents lists available at SciVerse ScienceDirect

Materials and Design

journal homepage: www.elsevier.com/locate/matdes

Prediction of flow stress in dynamic strain aging regime of austenitic stainless steel 316 using artificial neural network

Amit Kumar Gupta [a,*], Swadesh Kumar Singh [b], Swathi Reddy [c], Gokul Hariharan [d]

[a] Department of Mechanical Engineering, BITS-Pilani, Hyderabad Campus, AP 500 078, India
[b] Department of Mechanical Engineering, GRIET, Bachupally, Hyderabad, AP 500 072, India
[c] Research Scholar, Material Science and Engineering, University of New South Wales, Sydney 2052, Australia
[d] Department of Chemical Engineering, NIT, Warangal, AP 506 004, India

A R T I C L E I N F O

Article history:
Received 23 June 2011
Accepted 26 September 2011
Available online 1 October 2011

Keywords:
A. Ferrous metals and alloys,
E. Mechanical
F. Plastic behavior

A B S T R A C T

Flow stress during hot deformation depends mainly on the strain, strain rate and temperature, and shows a complex nonlinear relationship with them. A number of semi empirical models were reported by others to predict the flow stress during deformation. In this work, an artificial neural network is used for the estimation of flow stress of austenitic stainless steel 316 particularly in dynamic strain aging regime that occurs at certain strain rates and certain temperatures and varies flow stress behavior of metal being deformed. Based on the input variables strain, strain rate and temperature, this work attempts to develop a back propagation neural network model to predict the flow stress as output. In the first stage, the appearance and terminal of dynamic strain aging are determined with the aid of tensile testing at various temperatures and strain rates and subsequently for the serrated flow domain an artificial neural network is constructed. The whole experimental data is randomly divided in two parts: 90% data as training data and 10% data as testing data. The artificial neural network is successfully trained based on the training data and employed to predict the flow stress values for the testing data, which were compared with the experimental values. It was found that the maximum percentage error between predicted and experimental data is less than 8.67% and the correlation coefficient between them is 0.9955, which shows that predicted flow stress by artificial neural network is in good agreement with experimental results. The comparison between the two sets of results indicates the reliability of the predictions.

1. Introduction

Austenitic stainless steel 316 has been increasingly and extensively applied in the field of nuclear applications because of its excellent corrosion resistance in seawater environment due to having addition of molybdenum which prevents chloride corrosion. This steel is very useful in nuclear applications – particularly for cladding of fuel rods in the nuclear reactors. At elevated temperatures for specific strain rates under tensile load, the phenomenon of Dynamic Strain Aging (DSA) has been observed in this material. DSA is characterized by serrated stress–strain curve, i.e., wavy pattern like saw teeth on stress–strain curve. This is also called as Portevin-Le Chatelier (PLC) effect. This is due to the diffusion of solute atoms into mobile dislocations which temporarily get arrested at obstacles. The solute atoms are able to diffuse at a rate faster than the speed of the dislocations to catch and lock them. Therefore, due to the locked dislocations the load increases and when the dislocations are annihilated from the solute atoms, there is a sudden load drop. This process occurs many times, which causes serration in the stress–strain curve. Thus, DSA is manifested by a negative strain rate sensitivity, which results in unstable, jerky flow. DSA occurs for certain range of temperatures and strain-rates. A critical strain rate is required for serrated yielding to take place in a particular temperature range. This temperature range is called blue brittle region because metal heated to this temperature region shows a decrease in ductility and notch impact resistance. A widely accepted consequence of DSA is the negative strain rate sensitivity that is observed for many alloys.

Several researchers have studied the behavior of austenitic stainless steel under tension test to investigate the effect of temperature and strain rate on its mechanical properties [1–4]. Kaiping et al. [1] studied the serrated flow behavior of austenitic stainless steels in the different ranges of 523–673 K and 723–873 K at the strain rates of $5 \times 10^{-4}\,s^{-1}$. For these temperature–strain-rate combinations, a slow decrease in ultimate tensile strength and the negative strain rate sensitivity have been observed, which indicates the presence of DSA phenomenon in the material. The DSA pre-treatment can effectively improve the creep strength and the short-time tensile strength at high temperatures. Samuel et al. [2] observed increase in the ductile fracture resistance of titanium

* Corresponding author. Tel.: +91 40 66303518; fax: +91 40 66303998.
E-mail address: akgupta@bits-hyderabad.ac.in (A.K. Gupta).

0261-3069/$ - see front matter © 2011 Elsevier Ltd. All rights reserved.
doi:10.1016/j.matdes.2011.09.060

Table 1
Chemical composition of austenitic stainless steel 316 (wt.%).

Element	Fe	Cr	Ni	Mo	Mn	Si	Co	Cu
Composition (%)	67.690	16.630	10.850	2.420	1.280	0.380	0.210	0.210

Fig. 1. A computer controlled UTM with a high temperature chamber.

modified stainless steel due to DSA. The strengthening effect of DSA pre-treatment is much better than traditional cold-working pre-treatment. In a large number of metals and alloys, the DSA phenomenon alters the flow stress behavior of the metal and even it may cause the formation of flow-localized regions during deformation due to the negative strain rate sensitivity [5,6].

The flow stress during the hot deformation is influenced by many factors such as strain, strain rate and temperature etc. Due to the complex interconnections among these parameters and materials properties, mathematical models are sometimes very complex to handle by the numerical techniques as well as by experimental methods, especially when it involves some particular material phenomenon such as DSA. Considerable amount of work were done in past few decades to correlate the flow stress with the process parameters through the constitutive and the empirical models [7–16]. Cabrera et al. [7] determined the constitutive equations for the flow behavior of commercial Ti micro-alloyed steel. They conducted uniaxial hot compression tests over a wide range of strain rates (10^{-4}–$10\ s^{-1}$) and temperatures (1123–1423 K) and showed the inadequacy of the classical constitutive equations in taking the grain size into account. Chakravarty et al. [8] studied the characteristics of hot deformation of β-quenched Zr–2.5Nb–0.5Cu in the temperature range 650–1050 °C and in the strain rate range 0.001–100 s^{-1} using hot compression testing with the approach of processing maps and their interpretation through the Dynamic Materials Model. Cingara et al. [9] developed the constitutive equation relating peak stress, strain rate and temperature for hot working of 301, 304 and 317 steels using sinh equations. Laasraoui and Jonas [10] formulated the constitutive equations pertaining to idealized isothermal conditions for flow behavior of steels during deformation in the roll gap. Maheshwari et al. [11] used a modified Johnson–Cook (JC) material model to develop constitutive equations for hot deformation behavior of Al-2024 alloy. This empirical method depends on regression analysis to find the constants. The quantitative assessment of these models yields a wide range of errors which can go up to about 60% for a range of strain rates from (0.0001–100 s^{-1}). Many of the mechanisms of regression analysis do not describe the complex relationships of the various factors of flow stress with sufficient accuracy, because the effecting factors (strain, strain rate and temperature) of flow stress presents highly complicated non-linear interaction relationships during hot deformation. It is difficult to deal with the dispersed data through the regression method and also when a new experimental data is added, the regression constants need to be recalculated and moreover the regression method consumes a significantly longer time during computation. The research conducted by Guo and Sha [12], Malinov et al. [13] and Sun et al. [14] have mentioned the drawbacks concerning the development of constitutive relationship using conventional methods.

Recently artificial neural networks (ANN) have been applied for describing the hot deformation processes. The neural networks are a relatively new artificial intelligence technique that emulates the behavior of biological neural systems in digital software or hardware and this approach need not to have a well-defined process for algorithmically converting an input to an output. A significant advantage of the ANN approach is that one does not need to have a well-defined process for algorithmically converting an input to an output. Rather, it needs only a collection of representative examples of the desired mapping. The ANN then adapts itself to reproduce the desired output when presented with training sample input. Owing to their inherently high parallelism, ANN is ideally suited for the problem of estimating the flow stress from the available experimental data. ANN is the novel way to study the high temperature deformation behavior and some efforts have been made to the applications of ANN in some alloys. This model has good generalization performance without needing explicit mathematical and physical knowledge of deformation mechanism. The understanding of flow stress behavior in DSA regime becomes easier by using ANN modeling compared to modeling by constitutive equations.

Li et al. [15] established the predicting model for the calculation of flow stress of Ti-15–3 alloy based on the ANN method. Reddy

Table 2
Temperatures and strain rates in DSA region of austenitic stainless steel 316.

Temperatures (°C)	350	400	450	500	550	600	650
Strain rates (s^{-1})	10^{-4}	10^{-4} 10^{-3} 10^{-2}	10^{-4} 10^{-3} 10^{-2}	10^{-4} 10^{-3} 10^{-2}	10^{-4} 10^{-3} 10^{-2}	10^{-4} 10^{-3} 10^{-2}	10^{-4} 10^{-3} 10^{-2}

et al. [16,17] attempted to develop aback propagation neural network model to predict the flow stress of Ti–6Al–4V alloy for any given processing conditions. Kapoor et al. [18] used the ANN model to predict the deformation behavior of Zr–2.5Nb–0.5Cu, in the strain rate range of 10^{-3}–10 s^{-1}, temperature range of 650–1050 °C and strain range of 0.1–0.5. Singh and Gupta [19] developed an ANN model for predicting mechanical properties of extra deep drawn steel in the DSA regime. However, on the basis of ANN, little research work with regard to DSA region of austenitic stainless steel 316 was reported in the past years. Hence, in the present paper, constitutive relationship of austenitic stainless steel 316 in DSA regime was established using a feed-forward back-propagation ANN to asses flow stress. The input parameters are selected as strain, strain rate and temperature and the output parameter is flow stress. To construct ANN, tensile testing is done at different temperatures and strain rates and then the region of serrated flow is determined. The experimental data is divided into two parts. 90% data points are randomly selected as training data for training ANN and the remaining 10% data points are used as test data to evaluate the capability of the trained-up ANN. A good agreement is observed between the predicted results and the experimental data for test data that shows the reliability of the employed model.

2. Experimental details

The austenitic stainless steel 316 sheet with 1 mm thickness was used in this investigation. The composition of the employed material is given in Table 1. The samples were machined out of the raw material sheet by wire-cutting electro-discharge machining process for high accuracy and finish. Laboratory tensile tests were carried out to assess the flow stress behavior as well as to study the dynamic strain aging phenomenon. The tensile tests were performed using an indigenously developed universal testing machine (UTM) (as shown in Fig. 1) with capability of conducting tensile tests at elevated temperatures and constant strain rates. Four different true strain rates were used (10^{-4}, 10^{-3}, 10^{-2} and 10^{-1} s^{-1}) and various temperatures from room temperature to 650 °C at an interval of 50 °C. A computer control system is used to record the load versus displacement, which were converted into true stress versus true strain curves. Among all the conducted experiments, the strain rates and temperatures for the DSA region were identified, which are shown in Table 2. This data was used for preparing initial data for ANN as database. This data is divided into two sets; 90% data points are randomly selected as training data set for training ANN and the remaining 10% data points are used as test data set for testing the developed ANN.

3. Development of ANN model

Artificial neural network is a powerful data information treatment system which tries to simulate the neural networks structure of the human brain. It can represent and capture complex non-linear relationships between inputs and outputs. Each neural network is composed of an input layer, an output layer and one or more hidden layers, which are connected by the processing units called neurons. Each neuron works as an independent processing element, and has an associated transfer function, which describes how the weighted sum of its inputs is converted to the results into an output value. Currently, there are diverse training algorithms available. Among the various kinds of ANN approaches that have existed, the back propagation (BP) learning algorithm has become the most popular in engineering applications. Back propagation algorithm is based on minimization of the quadratic cost function by tuning the network parameters. The mean square error (MSE) is considered as a measurement criterion for a training set. Specially, BP neural network is the most suitable tool for treating non-linear systems.

Hence, a back propagation algorithm was applied to train a feed forward neural network, which is reliable and most commonly utilized. In this investigation, the input variables of ANN include stain, strain rate and deformation temperature, while the output variable is flow stress. Hence, a feed forward network trained with the back propagation algorithm was developed, as shown in Fig. 2. Before training the network, the input and output datasets have been normalized within the range of 0.05–0.95 to prevent a specific factor from dominating the learning for the ANN model. The main reason for normalizing the data matrix where the variables have been measured in different units is to recast them into the dimensionless units to remove the arbitrary effect of similarity between the objects. Thus, using Eq. (1), the experimental data was normalized to make the neural network training more efficient prior to the use of the datasets.

$$x_n = 0.05 + 0.90^*(x - x_{\min})/(x_{\max} - x_{\min}) \quad (1)$$

where $x_{\min}$ and $x_{\max}$ are the minimum and maximum values of x and x_n is the normalized data of the corresponding x. Once the best trained network is found, all the transformed data returns to their original value using the following equation:

$$x = x_{\min} + (x_n - 0.05)^*(x_{\max} - x_{\min})/0.9 \quad (2)$$

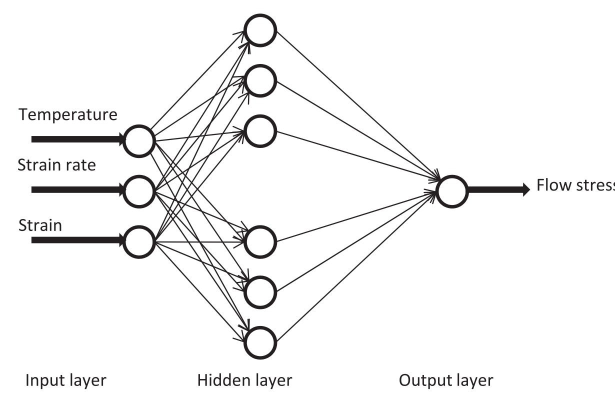

Fig. 2. Schematic illustration of the neural network architecture.

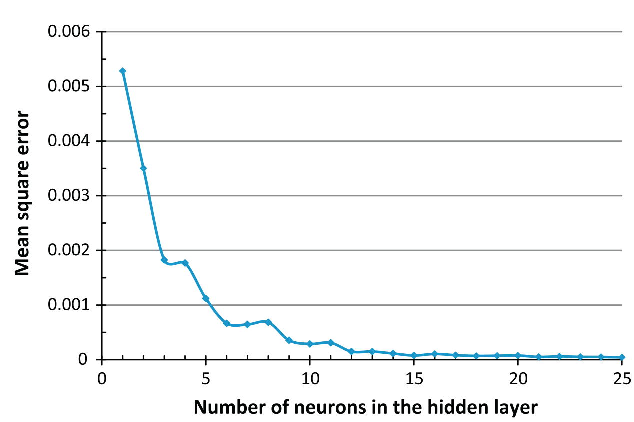

Fig. 3. Influence of hidden neutrons on the network performance.

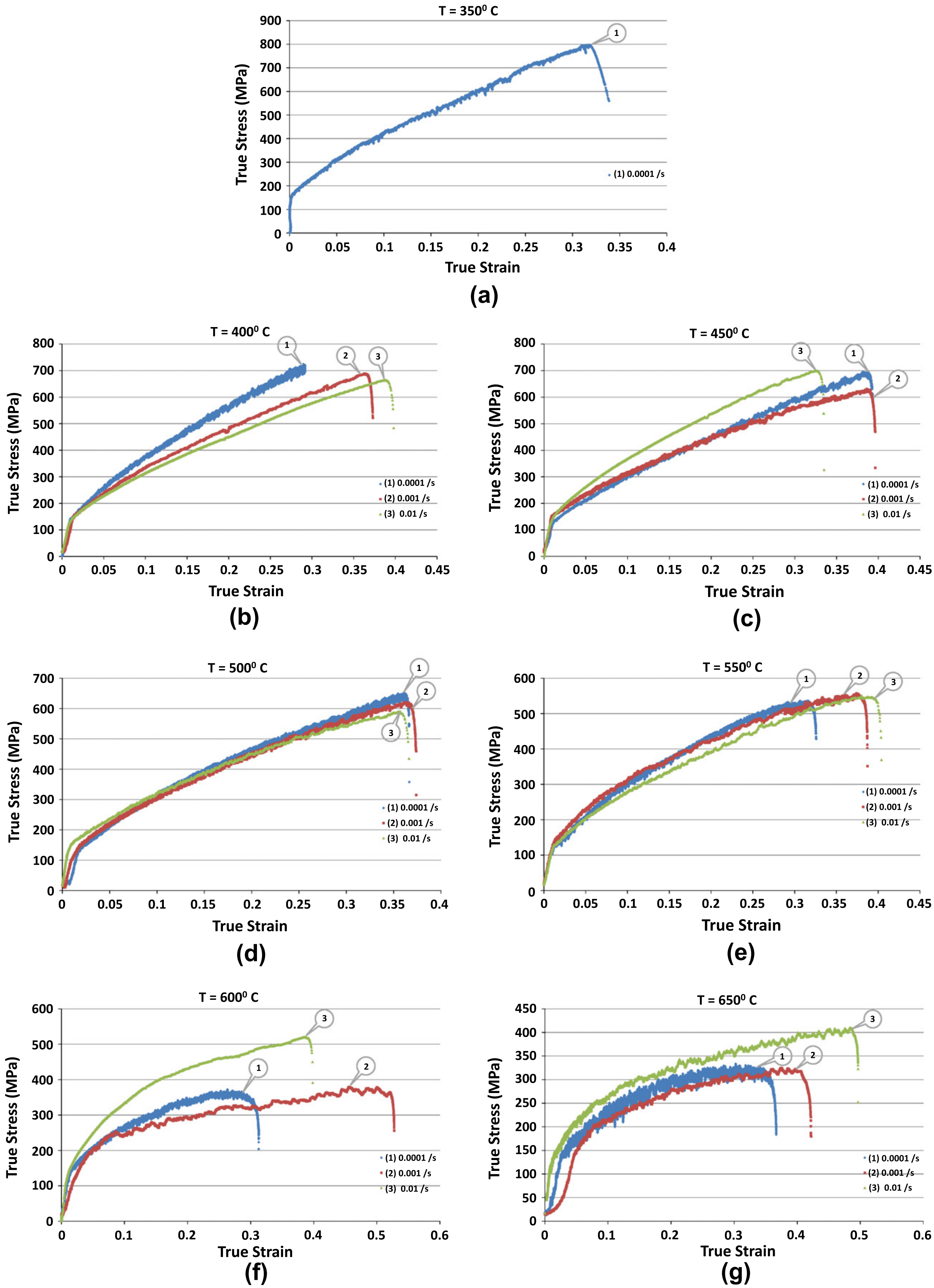

Fig. 4. True stress–true strain curves of austenite stainless steel 316 in DSA regime (a–g).

One of the most unresolved questions in the literature on ANN is what architecture should be used for a given problem. Architecture selection requires choosing both the appropriate number of hidden units and the connections thereof. The desirable network architecture contains as minimal as possible hidden units and connections necessary for a good approximation of the true function. In most of the applications of ANN, this selection was done using a trial-and-error procedure. The number of hidden layers determines the complexity of neural network and precision of predicted values. If the architecture is too complex, it may not converge during training or the trained data may be over fitted. In other way, the trained network might not have sufficient ability to learn the process correctly. Therefore, various network structures with varying number of neurons in hidden layer were examined. Fig. 3 shows the influence of number of neurons in hidden layer on the network performance. The value of mean square error (MSE) is used to check the ability of a particular architecture. It is observed that the mean square error of network decreases to the minimum value when the number of neurons is 15, which indicates that a network with 15 neurons in hidden layer can exhibit the best performance.

4. Results and discussion

Table 2 presents different temperatures and different strain rates at which the DSA phenomenon occurs in austenitic stainless steel 316. DSA occurrence is identified with the appearance of serrated flow in true stress–true strain curves, as shown in Fig. 4a–g. For the purpose of data analysis, the strains are selected from 0.02 to 0.30 at an interval of 0.01. Thus, total data points are 553, from which 90% data points (498) have been randomly selected as training dataset and the remaining 10% data points (55) have been taken as testing dataset. The correlation coefficient (R) is a commonly used statistic and provides information on the strength of linear relationship between experimental and predicted values. For perfect prediction, all the data points should lie on the line inclined at 45° from horizontal. Figs. 5 and 6 represent the predicted versus experimental flow stress values for the training and testing datasets respectively. In Fig. 5, the correlation coefficient is found to be 0.998, indicating that a very good correlation between experimental and predicted flow stress values has been obtained for the training dataset. Similarly, Fig. 6 shows the correlation coefficient to be 0.9955 for the testing dataset, indicating a very good correlation between experimental and predicted flow stress values. The results imply that the developed ANN model for austenitic stainless steel 316 are consistent with what is expected from fundamental theory of hot deformation, which suggests that the present model possesses excellent capability to predict the strain hardening and flow softening stages, especially in the DSA regime. Recently researchers [19,20] modeled DSA phenomenon using ANN and prediction of flow stresses was made very accurately. Singh and Gupta [19] also supported that ANN model can be applied to serrated flow and mechanical properties can be predicted very accurately once sufficient input data is calculated in the DSA region by experiments. Since in the present research 553 data points were calculated experimentally to model the ANN, flow stresses are predicted to some unknown temperature to a very close accuracy. This is also supported by Sheikh and Serajzadeh [20] in employing a neural network algorithm to assess flow stress of AA5083 in both regions of the serrated flow and the smooth yielding.

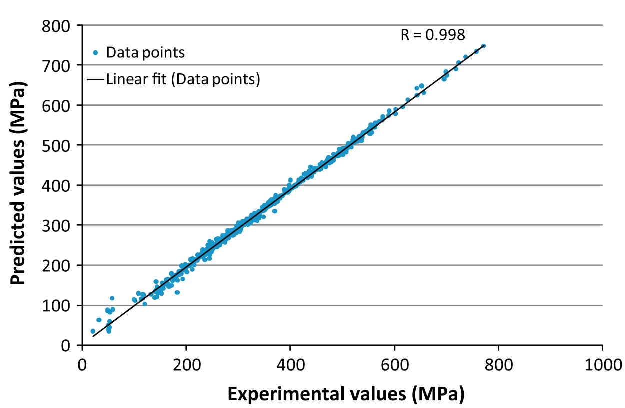

Fig. 5. Comparison between flow stress experimental and predicted values for the training dataset.

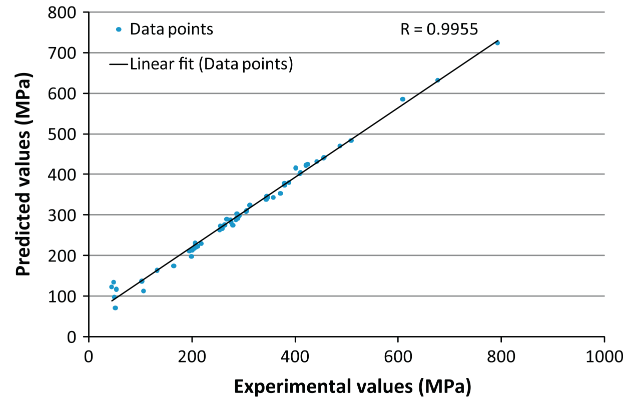

Fig. 6. Comparison between flow stress experimental and predicted values for the testing dataset.

Table 3 shows the experimental and ANN model predicted flow stress values along with the associated absolute and percentage errors for randomly selected unseen testing dataset. The maximum percentage error is found to be 8.67 with some exceptional cases (8, 9, 10, 36, 48, 49, 51 and 54 datasets as represented in Table 3 with bold and asterisk). It is observed that all these exceptional cases are found in the region where the experimental flow stress values are very low. Low flow stress values are associated with high temperature and low strain rate conditions [21,22]. As the temperature of the material increases there will be decrease in the mean flow stresses due to decrease in the work hardening region. The prediction of material properties and flow stresses are important in warm and hot forming to understand the behavior of any material during deformation and to finally model it for further stress analysis [21]. The evaluation of material properties required at a particular temperature is a time consuming process. As reported in the present research that at a very low strain rate ($0.0001\ s^{-1}$), it requires nine hours to conduct experiments on a servo hydraulic UTM. Test is required to calculate the parameters used in the constitutive equation at a particular temperature and the sensitivity index. It was also seen in the present investigation that once ANN model is developed all these parameters including the flow stresses required for simulation of warm forming [22] can be calculated at any unknown temperature. In DSA region the material properties behaves in a very unusual way. Depending on alloying element in the material like Cr (also in the present case) DSA region appears in certain temperature band which again increases the strength coefficient and work hardening exponent [19]. This happens to be on the boundary of the input domain. In general, the performance of any function fitting technique will be better, if more numbers of data are taken near the domain boundaries.

Table 3
Comparison of ANN predicted vs. experimental flow stress values for the testing dataset.

S. No.	Temperature	Strain rate	Strain	Flow stress (MPa) (experimental)	Flow stress (MPa) (predicted)	Absolute error	% Error
1	350	0.0001	0.08	379.7	373.09	6.61	1.740848
2	350	0.0001	0.21	609.15	585.98	23.17	3.803661
3	350	0.0001	0.24	677.33	632.6	44.73	6.603871
4	350	0.0001	0.31	792.95	724.17	68.78	8.673939
5	400	0.01	0.11	288.85	291.65	2.8	0.969361
6	400	0.0001	0.05	255.4	273.01	17.61	6.895067
7	400	0.0001	0.12	411.05	405.1	5.95	1.447512
8*	450	0.01	0.03	48.54	135.12	86.58	178.3684
9*	450	0.01	0.05	49.51	97.9	48.39	97.73783
10*	450	0.01	0.09	51.54	71.482	19.942	38.69228
11	450	0.001	0.07	267.75	289.67	21.92	8.186741
12	450	0.001	0.08	287.41	303.51	16.1	5.601754
13	450	0.001	0.1	312.34	324.19	11.85	3.793942
14	450	0.001	0.13	357.61	342.97	14.64	4.093845
15	450	0.001	0.14	372.01	353.78	18.23	4.900406
16	450	0.001	0.17	401.93	416.28	14.35	3.570273
17	450	0.001	0.18	424.8	425.34	0.54	0.127119
18	450	0.001	0.21	457.18	442.46	14.72	3.219738
19	450	0.001	0.26	509.03	484.38	24.65	4.842544
20	450	0.0001	0.18	421.04	422.85	1.81	0.429888
21	450	0.0001	0.19	442.35	431.84	10.51	2.375947
22	500	0.01	0.03	200.63	213.95	13.32	6.639087
23	500	0.01	0.15	388.55	380.05	8.5	2.187621
24	500	0.001	0.05	217.86	230.29	12.43	5.705499
25	500	0.001	0.07	254.27	263.58	9.31	3.661462
26	500	0.001	0.17	409.38	401.69	7.69	1.87845
27	550	0.01	0.05	204.66	218.63	13.97	6.825955
28	550	0.01	0.1	279.37	274.85	4.52	1.617926
29	550	0.01	0.19	379.7	379.1	0.6	0.158019
30	550	0.01	0.29	486.82	471.03	15.79	3.243499
31	550	0.001	0.05	211.93	223.32	11.39	5.374416
32	550	0.001	0.21	346.94	343.35	3.59	1.034761
33	550	0.001	0.22	345.37	346.72	1.35	0.390885
34	550	0.0001	0.05	206.31	224.06	17.75	8.603558
35	550	0.0001	0.09	285.18	288.36	3.18	1.115085
36*	600	0.01	0.01	132.36	164.04	31.68	23.93472
37	600	0.01	0.24	455.87	441.06	14.81	3.248733
38	600	0.001	0.16	274.53	288.42	13.89	5.059556
39	600	0.001	0.24	305.36	309.47	4.11	1.345952
40	600	0.0001	0.1	263.75	275.89	12.14	4.602844
41	600	0.0001	0.22	344.36	338.13	6.23	1.809153
42	650	0.01	0.01	106.27	112.59	6.32	5.947116
43	650	0.01	0.03	165.04	174.59	9.55	5.786476
44	650	0.01	0.11	259.37	266.62	7.25	2.795235
45	650	0.01	0.16	287.43	293.64	6.21	2.160526
46	650	0.01	0.17	292.15	298.52	6.37	2.180387
47	650	0.01	0.2	306.86	310.73	3.87	1.261161
48*	650	0.001	0.03	53.39	117.26	63.87	119.6291
49*	650	0.001	0.04	102.96	137.07	34.11	33.12937
50	650	0.001	0.08	198.98	198.11	0.87	0.43723
51*	650	0.0001	0.01	44.41	123.18	78.77	177.37
52	650	0.0001	0.07	195.34	211.54	16.2	8.293232
53	650	0.0001	0.08	209.18	222.06	12.88	6.157376
54*	650	0.0001	0.09	206.15	231.75	25.6	12.41814
55	650	0.0001	0.16	276.37	282.37	6	2.171003

5. Conclusions

In the present study, the flow stress of austenitic stainless steel 316 is predicted using artificial neural networks with regard to dynamic strain aging that occurs in certain deformation conditions and varies flow stress behavior of metal being deformed. The constitutive relationship of the austenitic stainless steel 316 alloy is successfully established using the ANN model based on experimental results from the hot tensile testing. In the developed ANN model, the inputs are strain, strain rate and deformation temperature, whereas flow stress is the output. After testing the effect of number of neurons in the hidden layer on the network performance, the optimal configuration of the ANN model using BP algorithm was found to be 3–15−1. The neural network based model clearly indicates that it can be learned from the training dataset and able to predict accurately the output of unseen testing dataset. The maximum percentage error for the testing dataset is found to be 8.67%, and the correlation coefficient is 0.9955. From this it can be concluded that well-trained artificial neural network models provide fast, accurate and consistent results, making them superior to the conventional constitutive models, especially in the DSA regime of austenitic stainless steel 316.

Acknowledgements

The financial support received for this research work from Department of Atomic Energy (DAE), Government of India, through

Young Scientist Research Award 2009/36/45-BRNS/1751 is gratefully acknowledged.

References

[1] Kaiping P, Kuangwu Q, Wenzhe C. Effect of dynamic strain aging on high temperature properties of austenitic stainless steel. Mater Sci Eng A 2004;379:372–7.
[2] Samuel KG, Ray SK, Sasikala G. Dynamic strain ageing in prior cold worked 15Cr–15Ni titanium modified stainless steel (Alloy D9). J Nucl Mater 2006;355(1–3):30–7.
[3] Armas AF, Bettin OR, Alvarez-Armas I, Rubiolo GH. Strain aging effects on the cyclic behavior of austenitic stainless steels. J Nucl Mater 1988;155–157:644–9.
[4] Jiang H, Chen X, Fan Z, Dong J, Jiang H, Lu S. Influence of dynamic strain aging pre-treatment on creep-fatigue behaviour in 316L stainless steel. Mater Sci Eng A 2009;500(1–2):98–103.
[5] Klose FB, Ziegenbein A. Analysis of Portevin-Le Chatelier serrations of type Bin Al–Mg. Mater Sci Eng A 2004;369:76–81.
[6] Pink E, Kumar S. Serrated flow of aluminum alloys influenced by precipitates. Mater Sci Eng A 2000;280:17–24.
[7] Cabrera JM, Al Omar A, Jonas JJ, Prado JM. Modeling the flow behavior of a medium carbon micro alloyed steel under hot working conditions. J Metall Mater Trans A: Phys Metall Mater Sci 1997;11:2233–44.
[8] Chakravarty JK, Dey GK, Banerjee S, Prasad YVRK. Characterization of hot deformation behavior of Zr–2.5Nb–0.5Cu using processing maps. J Nucl Mater 1995;218(2):247–55.
[9] Cingara A, McQueen HJ. New method for determining sinh constitutive constants for high temperature deformation of 300 austenitic steels. J Mater Process Technol 1992;36:17–30.
[10] Laasraoui A, Jonas JJ. Prediction of steel flow stresses at high temperatures and strain rates. Metall Trans A 1991;22:1545–58.
[11] Maheshwari AK, Pathak KK, Ramakrishnan N, Narayan SP. Modified Johnson–Cook material flow model for hot deformation processing. J Mater Sci 2010;45(4):859–64.
[12] Guo Z, Sha W. Modeling the correlation between processing parameters and properties of maraging steels using artificial neural network. Comput Mater Sci 2004;29:12–28.
[13] Malinov S, Sha W, Mckeown JJ. Modeling the correlation between processing and properties in titanium alloys using artificial neural network. Comput Mater Sci 2001;21:375–94.
[14] Sun Y, Zeng WD, Zhao YQ, et al. Development of constitutive relationship model of Ti600 alloy using artificial neural network. Comput Mater Sci 2010;48:686–91.
[15] Li P, Xue KM, Lu Y, Tan JR. Neural network prediction of flow stress of Ti-15–3 alloy under hot compression. J Mater Process Technol 2004;148:235–8.
[16] Reddy NS, Lee YH, Kim JH, Lee CS. High temperature deformation behavior of Ti–6Al–4V alloy with and equiaxed microstructure: a neural networks analysis. Met Mater Int 2008;14(2):213–21.
[17] Reddy NS, Lee YH, Parka CH, Lee CS. Prediction of flow stress in Ti–6Al–4V alloy with an equiaxed a + b microstructure by artificial neural networks. Mater Sci Eng A 2008;492:276–82.
[18] Kapoor R, Pal D, Chakravarty JK. Use of artificial neural networks to predict the deformation behavior of Zr–2.5Nb–0.5Cu. J Mater Process Technol 2005;169:199–205.
[19] Singh SK, Gupta AK. Prediction of mechanical properties of extra deep drawn steel in blue brittle region using artificial neural network. Mater Des 2010;31:2288–95.
[20] Sheikh H, Serajzadeh S. Estimation of flow stress behavior of AA5083 using artificial neural networks with regard to dynamic strain ageing effect. J Mater Process Technol 2008;196:115–9.
[21] Singh SK, Gupta AK, Mahesh K. A study on the extent of ironing of EDD steel at elevated temperature. CIRP J Manuf Sci Technol 2010;3(1):73–9.
[22] Singh SK, Swathi M, Kumar A, Mahesh K. Understanding formability of EDD steel at elevated temperatures using finite element simulation. Mater Des 2010;31:4478–84.